O-Glycosylated Human MUC1 Repeats Are Processed In Vitro by Immunoproteasomes

Tanja Ninkovic and Franz-Georg Hanisch

J Immunol 2007; 179:2380-2388; ;
doi: 10.4049/jimmunol.179.4.2380
http://www.jimmunol.org/content/179/4/2380

The Journal of Immunology is published twice each month by
The American Association of Immunologists, Inc.,
1451 Rockville Pike, Suite 650, Rockville, MD 20852

Print ISSN: 0022-1767 Online ISSN: 1550-6606.

O-Glycosylated Human MUC1 Repeats Are Processed In Vitro by Immunoproteasomes[1]

Tanja Ninkovic* and Franz-Georg Hanisch[2]*†

The targeting of epitopes on tumor-associated glycoforms of human MUC1 represents a primary goal in immunotherapeutic anticancer strategies. Effective immune responses to cancer cells certainly require the activation of specific cytotoxic T cell repertoires by cross-priming of dendritic cells either via immunoproteasomal or by endosomal processing of ectodomain epitopes on MUC1-positive carcinomas. Because no evidence is currently available on the capacities of human immunoproteasomes to cleave mucin-type *O*-glycosylated peptides, we performed in vitro studies to address the questions of whether glycosylated MUC1 repeats are cleaved by immunoproteasomes and in which way *O*-linked glycans control the site specificity of peptide cleavage via their localization and structures. We show for the first time that mucin-type *O*-glycosylated peptides are effective substrates of immunoproteasomes, however, the patterns of cleavage are qualitatively and quantitatively influenced by *O*-glycosylation. The nonglycosylated MUC1 repeat peptide (clusters of oligorepeats AHGVTSAPDTRPAPGSTAPP or AHGVTSAPESRPAPG STAPA) is cleaved preferentially within or adjacent to the SAP and GST motifs with formation of a complex fragment pattern that includes major nona- and decapeptides. *O*-GalNAc modified peptides are largely resistant to proteolysis if these preferred cleavage sites are located adjacent to *O*-glycosylation, whereas peptides even with elongated glycans at more distant sites can form effective substrates yielding major glycopeptide fragments in the class I size range. ***The Journal of Immunology,*** **2007, 179: 2380–2388.**

Research over three decades has revealed a series of tumor target Ags with proven potential in clinical diagnostics or in immunotherapy. Among these are the carcinoembryonic Ag, the ovarian carcinoma marker CA125 (MUC16), and the epithelial tumor markers MUC1 and HER2neu. A common feature of the epithelial tumor markers is that they belong to the family of glycoproteins. MUC1 represents a heavily *O*-glycosylated type 1 transmembrane mucin that is expressed in most epithelial and some nonepithelial tissues on the apical surfaces of polarized cells (1). Due to the luminal topology in many glandular and ductal epithelia, it remains largely inaccessible for the immune system under normal conditions, a fact which may explain its moderate immunogenicity in lactating women and cancer patients having small amounts of shed or secreted MUC1 in their circulation (2). In most carcinomas, the mucin is strongly overexpressed, and displays aberrant *O*-glycosylation with mainly short glycan chains (GalNAc, Galβ1-3GalNAc, and NeuAcα2-3Galβ1-3GalNAc), which correspond to the well-established, cancer-associated glycoepitopes Tn, TF, or sialyl-TF (3). Moreover, with the loss of polarity, carcinoma cells express MUC1 epitopes in a pericellular fashion, making the several hundred nanometer-long ectodomain of the mucin a primary immune target in anticancer strategies. On top of these features, the major immunodominant epitopes on cancer-associated MUC1 glycoforms are found in many copies per molecule due to their location in a tandem repeat domain. This domain comprises up to 120 repetitions of a 20-meric peptide in clusters of two variant sequences (HGVTSAPDTR PAPGST APPA or HGVTSAPESRPAPGSTAPA) containing five potential *O*-glycosylation sites (4).

It was earlier noticed that CTL derived from patients with breast carcinoma recognize an epitope present on MUC1 tandem repeat peptide (5) pointing to the potential application of the Ag in immunotherapeutic strategies. This MHC-unrestricted epitope localizes to the DTR motif within the MUC1 tandem repeat and represents also the major target of B cell responses in humans and mice. A few MHC-restricted T cell epitopes present on MUC1 have been identified so far. Among these the STAPPAHGV sequence of the tandem repeat was shown to bind strongly to HLA-A11, and to a lesser extent to HLA-A1, A2.1, and A3 (6). Two other HLA-A2-restricted T cell epitopes localize within and outside of the tandem repeat domain (7). One corresponds to the sequence STAPPVHNV within degenerate repeats that C-terminally flank the repeat domain. The second, with the sequence LLLLTV LTV, is located within the signal peptide of MUC1, indicating that T cell responses to the mucin are not restricted to the repeat domain. Further examples of ectodomain epitopes outside of the repeat domain were identified as the HLA-A2-restricted sequences TLAPATEPA (N-terminal of the repeat domain), FLSFHISNL (C-terminal of the repeat domain), and ALGSTAPPV or SAPDNR PAL (C-terminal degenerate repeats) (8, 9).

Initial attempts to induce class I-restricted CTL responses revealed that presentation of the Ag by dendritic cells (DCs)[3] and CTL function correlated negatively with the degree of glycosylation (10). A similar unresponsiveness to tumor-associated glycoforms of the mucin was also found in the MHC class II pathway

*Center of Biochemistry, Medical Faculty, and †Center for Molecular Medicine Cologne, University of Cologne, Köln, Germany

Received for publication January 18, 2007. Accepted for publication June 11, 2007.

The costs of publication of this article were defrayed in part by the payment of page charges. This article must therefore be hereby marked *advertisement* in accordance with 18 U.S.C. Section 1734 solely to indicate this fact.

[1] This work was supported by National Institutes of Health Grant 1RO1 CA84106 (to F.-G.H.) and by the Köln-Fortune Programme (to F.-G.H.).

[2] Address correspondence and reprint requests to Dr. Franz-Georg Hanisch, Institute of Biochemistry II, Medical Faculty, University of Cologne, Joseph-Stelzmann-Strasse 52, 50931 Köln, Germany. E-mail address: franz.hanisch@uni-koeln.de

[3] Abbreviations used in this paper: DC, dendritic cell; ER, endoplasmic reticulum; TFA, trifluoroacetic acid; ESI, electrospray ionization; Gal, galactose; GalNAc, *N*-acetylgalactosamine; LC, liquid chromatography; MS, mass spectrometry.

and could be assigned to multivalent carbohydrate-lectin interactions in early endosomes (11). We previously showed that short *O*-linked glycans, like GalNAc or Gal1-3GalNAc, on MUC1 tandem repeats remain intact during DC processing in the MHC class II pathway (12), that they control the extent and site specificity of cathepsin L-mediated endosomal proteolysis of MUC1 glycopeptides (13), and are able to elicit peptide or mixed glycopeptide specific Th cell responses (12). Moreover, there is evidence that MUC1 glycopeptides can bind more strongly to the MHC class I mouse allele $H2k^b$ compared with the corresponding unglycosylated peptide (14) and induce activation of CTL in human MUC1/HLA-A*0201-transgenic mice (15).

Nothing is known, however, about the mechanisms by which the ectodomain of the mucin gets access to the processing active enzymes in the MHC class I pathway. Cross-priming by APCs can occur due to two possible routes of processing after endocytosis of topologically extracellular Ag, phagocytosis or macropinocytosis. One possibility is that endosomal Ag escapes into the cytosol, where it reaches immunoproteasomes and other cytosolic enzymes (16, 17). Alternatively, Ag is processed in endosomes by cathepsins residing there (18, 19). Both of these pathways can generate 8- to 11-meric peptides potentially fitting to the groove of MHC class I molecules.

Proteasomes are multisubunit proteinases involved in the breakdown of both misfolded and regulatory cellular proteins (20). Immunoproteasomes are a type of proteasomes expressed in APCs under the influence of IFN-γ, which have three subunits changed to special immunosubunits (21). It is known that immunoproteasomes and constitutive proteasomes show different processing patterns (22). Cellular proteins that are targets of proteasomes are often glycosylated by *N*- and/or *O*-linked glycosylation. It is believed that deglycosylation of such proteins is a prerequisite for subsequent proteolysis by the proteasome, because bulky glycan chains may impair their efficient entry into the interior of the cylinder-shaped proteasome. This is confirmed by the finding that no *N*-glycosylated peptides were found presented on the cell surface in MHC class I/peptide complexes (23). Apparently, these peptides require PNGase activity and retrograde endoplasmic reticulum (ER) transport for presentation as exemplified for a tyrosinase epitope (24). In contrast to *N*-glycopeptides, it is still not clear, how efficiently proteasomes process *O*-glycosylated peptides. Haurum et al. and colleagues (25–27) were the first who studied intracellular processing and presentation of *O*-β-GlcNAc-glycopeptides, a protein modification that, according to current knowledge, is not elongated like mucin-type *O*-glycans, and introduced exclusively into nucleocytosolic proteins on a substoichiometric level. *O*-β-GlcNAc modified peptides act as suitable substrates for TAP-mediated transport into the ER (27), were isolated from MHC class I/peptide complexes on cell surfaces (26), and demonstrated to elicit glycopeptide-specific CTL responses in mice (25). This implies that *O*-GlcNAc-modified proteins are processed by proteasomes without prior deglycosylation by a cytosolic β-glycosaminidase. However, none of these studies have addressed whether mucin-type glycosylated proteins are suitable substrates of immunoproteasomes and whether MHC class I epitopes can be generated by this processing.

We have performed in vitro studies simulating the processing of MUC1-derived glycopeptides by immunoproteasomes. Because GalNAc and Gal1-3GalNAc have been shown to survive the endosomal processing and no cytosolic glycosidases are known, which could trim mucin-type glycans, these core-type glycans represent true proteasomal substrates. After in vitro proteolysis, separation of fragments by HPLC and their analysis by mass spectrometry, immunoproteasomes were shown in this study to process *O*-glycosylated MUC1 glycopeptides that carried GalNAc or Gal1-3GalNAc. However, efficacy and site specificity of proteolysis were strongly influenced by *O*-glycosylation. Processing efficacy was dependent on the density and site of *O*-glycosylation, the glycosylation type, and peptide sequence variations.

Materials and Methods

Immunoproteasomes

Incorporation of the IFN-γ-inducible subunits low m.w. proteins -2 and -7, and the multicatalytic endopeptidase complex-like-1 leads to the formation of immunoproteasomes (i20S), which are associated with more efficient class I Ag processing than constitutive proteasomes (c20S). The 20S proteasomes were isolated according to previously published protocols (28) using frozen pellets of LCL-721 cells, which were lysed in a buffer containing 0.1% Triton X-100 on ice and homogenized in a Dounce homogenizer. The 40,000 × *g* supernatant of the lysate was bound to DEAE-52-Servacel (Serva), and the eluted fraction (300 mM NaCl) was precipitated with 30–70% $(NH_4)_2SO_4$. The precipitate was dissolved in low salt buffer and subjected to fast protein anion exchange chromatography with 100 ml of TSK-DEAE-650 S Toyopearl resin (Tosohaas) in a HR 16/60 column (Amersham Pharmacia Biotech). Proteins were eluted with a gradient (80–250 mM NaCl in 250 min at a flow rate of 2 ml/min). Protease-active fractions were pooled, concentrated, and loaded onto a 10–35% glycerol gradient. After centrifugation at 100,000 × *g* for 18 h (Beckman Ultracentrifuge Optima L-80, SW40 Ti), gradient fractions were tested for protease activity. The purity of the proteasome preparations was checked by SDS-PAGE combined with Coomassie staining and revealed to be >95%. The content of c20S in the i20S preparation was estimated on the basis of the constitutive subunit β5. Western blot analysis and mass spectrometry of β5 vs β5i peptides revealed that the i20S preparation did not contain >10% c20S proteasomes. A 1 mg/ml solution of immunoproteasomes prepared according to the above-outlined protocol was purchased from Immatics Biotechnologies and stored frozen at −80°C.

Peptides and glycopeptides

To ensure that the glycopeptides used in this study represent substrates, which closely resemble tumor-associated MUC1, their *O*-glycan substitution was designed in accordance with well-established glycoprofiles on breast cancer cells. These cells express preferentially core 1-based glycans, Tn, TF, and the respective sialylated derivative corresponding to GalNAc, Galβ1-3GalNAc, and NeuAcα2-3Galβ1-3GalNAc, respectively (3). MUC1-derived glycopeptides were chemically synthesized and provided by Prof. H. Paulsen (Institute of Organic Chemistry, University of Hamburg, Hamburg, Germany) (GP1–16; GGP1–4; SGGP1–5). The 100-mer peptide (P1 in Table I) and 61-mer (P2 in Table I) was provided by Prof. O. Finn (Department of Immunology, University of Pittsburgh School of Medicine, Pittsburgh, PA) and in vitro glycosylated with GalNAc using purified polypeptide GalNAc-transferases T1 and T2 (provided by Dr. H. Clausen, School of Dentistry, University of Copenhagen, Copenhagen, Denmark) under conditions described previously (29, 30). Other nonglycosylated peptides were ordered from Mimotopes/Perbio and glycosylated in vitro. TAP25 was synthesized in a local facility at the Institute of Biochemistry (Cologne, Germany). All (glyco)peptides were purified by HPLC and finally checked for the degree of purity, which was above 98%.

In vitro assays with human immunoproteasomes

Ten micrograms of each peptide or glycopeptide were incubated with 1 μg of human 20S immunoproteasomes (Immatics) for 48 h, at 37°C, in 10 μl of digestion buffer. Three different buffer systems were tested: buffer A: 50 mM Tris-HCl, 25 mM KCl, 10 mM NaCl, 1 mM $MgCl_2$, 1 mM DTT; buffer B: 20 mM HEPES/KOH (pH 7.6) containing 2 mM $Mg(CH_3COO)_2$; and buffer C: 20 mM HEPES/KOH (pH 7.6) containing 2 mM $Mg(CH_3COO)_2$ and 1 mM DTT (Fig. 1). Buffer B was used in assays with nonglycosylated peptides, buffer C with glycosylated peptides. Digestion was stopped by freezing the sample at −80°C when nonglycosylated reference peptide P1 (100-mer) was completely cleaved.

Proteasome purity was controlled by inhibition of immunoproteasome-specific activity with the proteasome inhibitor Ada(Ahx)3-(Leu)3-Vinyl sulfone (150 μM; Biomol) in 10 μl of digestion buffer B. A preincubation of human 20S immunoproteasomes (1 μg) with inhibitor for 10 min at room temperature was followed by addition of 10 μg of P1 peptide and incubation at 37°C for 24 h to check for contaminating proteolytic activity. Under these conditions, no proteolytic degradation was detectable and contaminating protease and peptidase could hence be excluded (Fig. 2).

Table I. *Quantitative analysis of processing rates measured in vitro with human immunoproteasomes and MUC1 (glyco)peptides*[a]

	Designation	Peptide Sequence and Sites of *O*-Glycosylation	Processing Rate (%)
Peptides	P1 (HGV100)	(GVTSAPDTRPAPGSTAPPAH)$_5$	100
	P2 (AHG61)	A(HGVTSAPESRPAPGSTAPPA)$_3$	100
	P3 (AHG21-DTR)	AHGVTSAPDTRPAPGSTAPPA	100
	P4 (AHG21-ESR)	AHGVTSAPESRPAPGSTAPPA	100
GalNAc-glycopeptides	GP1 (HGV100-G_3-V**T**S,S**T**A)	(HGV**T**SAPDTRPAPG**ST**APPA)$_5$	<1
	GP2 (AHG21-G_1-V**T**S)	AHGV**T**SAPDTRPAPGSTAPPA	57
	GP3 (AHG21-G_1-D**T**R)	AHGVTSAPD**T**RPAPGSTAPPA	94
	GP4 (AHG21-G_1-S**T**A)	AHGVTSAPDTRPAPGS**T**APPA	63
	GP5 (AHG21-ES-G_1-V**T**S)	AHGV**T**SAPESRPAPGSTAPPA	65
	GP6 (AHG21-ES-G_1-E**S**R)	AHGVTSAPE**S**RPAPGSTAPPA	74
	GP7 (AHG21-ES-G_1-S**T**A)	AHGVTSAPESRPAPGS**T**APPA	64
	GP8 (AHG21-G_1-T**S**A)	AHGVT**S**APDTRPAPGSTAPPA	70
	GP9 (SAP20-G_2-**S**AP,S**T**A)	**S**APDTRPAPGS**T**APPAHGVT	54
	GP10 (SAP20-G_2-**S**AP,D**T**R)	**S**APD**T**RPAPGSTAPPAHGVT	54
	GP11 (SAP20-G_3-**S**APD**T**R,S**T**A)	**S**APD**T**RPAPGS**T**APPAHGVT	65
	GP12 (SAP20-G_1-D**T**R)	SAPD**T**RPAPGSTAPPAHGVT	56
	GP13 (SAP20-G_2-D**T**R,S**T**A)	SAPD**T**RPAPGS**T**APPAHGVT	74
	GP14 (SAP20-G_1-S**T**A)	SAPDTRPAPGS**T**APPAHGVT	68
	GP15 (HGV20-G_2-V**T**S,S**T**A)	HGV**T**SAPDTRPAPGS**T**APPA	<1
	GP16 (HGV20-G_5)	HGV**TS**APD**T**RPAPG**ST**APPA	<1
Gal-GalNAc-glycopeptides	GGP1 (AHG21-GG_1-V**T**S)	AHGV**T**SAPDTRPAPGSTAPPA	91
	GGP2 (AHG21-GG_1-D**T**R)	AHGVTSAPD**T**RPAPGSTAPPA	89
	GGP3 (AHG21-GG_1-S**T**A)	AHGVTSAPDTRPAPGS**T**APPA	88
	GGP4 (AHG21-GG_1-T**S**A)	AHGVT**S**APDTRPAPGSTAPPA	86
NeuAc-Gal-GalNAc-glycopeptides	SGGP1 (AHG21-SGG_1-V**T**S)	AHGV**T**SAPDTRPAPGSTAPPA	<1
	SGGP2 (AHG21-SGG_2-VT**S**)	AHGV**TS**APDTRPAPGSTAPPA	<1
	SGGP3 (AHG21-SGG_2-S**T**A)	AHGVTSAPDTRPAPG**ST**APPA	<1
	SGGP5 (AHG21-SGG_5)	AHGV**TS**APD**T**RPAPG**ST**APPA	<1

[a] Synthetic peptides and glycopeptides were incubated with human immunoproteasomes and the digestion products were chromatographed by reverse-phase HPLC for quantification of the relative amounts of residual substrate. Peptides are named systematically starting with P followed by a running number, glycopeptides substituted with the monosaccharide GalNAc by the designation GP, those substituted with the disaccharide Gal-GalNAc or the trisaccharide NeuAc-Gal-GalNAc by GGP or SGGP, respectively. These designations are followed by a second systematic designation, which defines also the starting motif and length of the peptide, the number and type of glycans, and the sites of glycan substitution. The glycosylated amino acids are labeled with bold underlined letters.

Prediction of proteasome digestion pattern

Sequences of oligomeric MUC1 repeat peptides were submitted to analyses by the NetChop 3.0 server producing neural network predictions for cleavage sites of proteasomes. The bioinformatic tool is available at the internet portal of the Centre for Biological Sequence Analyses (Technical University of Denmark, Lynby, Denmark; www.cbs.dtu.dk/services/NetChop/). The prediction method C-term 3.0 with a threshold of 0.5 was used.

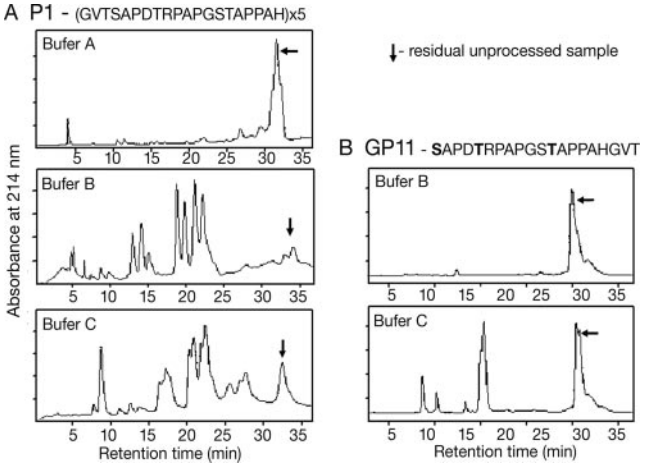

FIGURE 1. Influence of buffer conditions on processing efficiency. Digestion of P1 peptide and GP11 glycopeptide was performed in three different buffer systems and the products were analyzed by HPLC. *A*, Processing of nonglycosylated 100-mer P1 was slow in buffer A, most effective in buffer B (without DTT). *B*, Processing of glycopeptides was more effective in the presence of DTT (buffer C).

Quantitative HPLC analysis

Each sample was analyzed by reverse-phase HPLC on a Beckman Coulter Ultrasphere ODS 2 μm column (150 × 2 mm), using a flow rate of 0.3 ml/min and a linear gradient of solvent A (2% acetonitrile in aqueous 0.1% trifluoroacetic acid (TFA)) and solvent B (80% acetonitrile in aqueous 0.1% TFA) increasing from 6 to 26 or 6–36% solvent B during 30 min, with a final wash for 10 min with solvent B. The eluate was monitored by UV detection at 214 nm. Fractions were collected manually, dried by vacuum centrifugation, dissolved in 5 μl of 0.1% aqueous TFA and subsequently analyzed by positive ion MALDI-TOF mass spectrometry (MS) and/or by nano-liquid chromatography (LC)/electrospray ionization (ESI)-MS/MS spectrometry for obtaining sequence data. Peptide quantities in each HPLC fraction were calculated as relative peak areas using the Beckman Gold software.

MS analyses

MALDI-MS. The glycopeptide or peptide samples were applied as 0.1% TFA solutions and mixed 1:2 with the matrix 1,5-dihydroxybenzoic acid (saturated solution in acetonitrile/0.1% TFA, 1:2). After cocrystallization of analyte and matrix, the spots were analyzed on a Bruker Reflex IV instrument (Bruker Daltonik) by positive ion detection in the reflectron mode. Ionization of cocrystallized analytes was induced with a pulsed nitrogen laser beam (337 nm) and the ions were accelerated in a field of 20 kV and reflected at 23 kV.

LC/ESI-MS. Nanoflow LC with online ESI-MS was performed on a Q-TOF2 quadrupole-time-of-flight mass spectrometer (Waters) equipped with a Z spray source. Samples were introduced using the Ultimate nano-LC system (LC-Packings) equipped with the Famos autosampler and the Switchos column-switching module. The column setup comprised a 0.3 × 10-mm trap column and a 0.075 × 150-mm analytical column, both packed with 3-μm PepMap C18 (LC-Packings). The analytical column flow rate was ~200 nl/min, resulting from a 1:1,000 split of the 200-μl/min flow delivered by the system pump. The samples were eluted onto the analytical column by using a gradient of acetonitrile in 0.1% formic acid over 30 min.

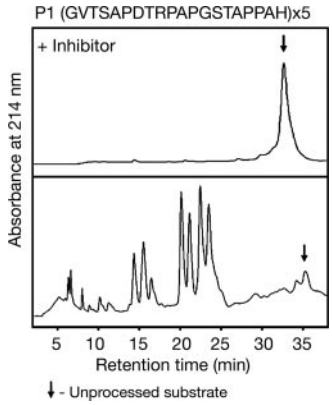

FIGURE 2. The immunoproteasomes did not exhibit contaminating nonproteasomal proteolytic activity. The peptide substrate P1 (100-mer) was processed by human immunoproteasomes in buffer B with (*upper panel*) or without (*lower panel*) the proteasome inhibitor. Digests were fractionated by reverse-phase HPLC and fractions analyzed by MALDI-MS. No immunoproteasome-independent proteolytic activity was detectable in the presence of inhibitor.

Computer analyses of peptide fragments

The ions detected by MALDI-MS were analyzed by the FindPep software application from ExPASy Proteomic server of Swiss Institute of Bioinformatics: www.expasy.org/tools/findpep.html. The software can identify peptides that result from unspecific cleavage of proteins from their experimental masses, taking into account chemical modifications, posttranslational modifications and protease autolytic cleavage. The experimentally measured peptide masses are compared with the theoretical peptides calculated from a user-entered sequence or from a specified Swiss-Prot/TrEMBL entry, with the deviation settled to ± 1 Da.

Determination of cleavage frequencies at individual peptide bonds

Determination of the cleavage frequencies at individual peptide bonds of the substrates was based on the identification and quantification of proteolytic products. Quantification was performed in a two-step process by first measuring the relative areas of individual peptide-containing HPLC peaks within a chromatogram, followed by estimating the relative ion intensities of individual peptide signals registered by MS for each HPLC peak. Although desorption ionization in MALDI-MS can give only approximative values for the relative amounts of an analyte in a mixture due to suppression effects caused by easily desorbing components, reliable data can be obtained for mixtures of low complexity and for compounds of similar size and polarity. This prerequisite was fulfilled for peptides within individual HPLC fractions, which contained generally one to four peptide species with closely related structures (partially overlapping sequences) and expectedly similar desorption efficiencies in MALDI-MS.

Results

Immunoproteasomes process glycopeptides in vitro, but dependent on the glycosylation sites

A systematic study of processing efficiency by immunoproteasomes covered a size range of glycopeptide and peptide substrates varying from 20 to 100 aa. The substrates represented sections of the MUC1 tandem repeat domain with different starting motifs within the repeat (AHG or SAP) and were *O*-glycosylated similar to tumor-associated MUC1 with single or multiple GalNAc (Tn Ag), Galβ1-3GalNAc (TF Ag), or NeuAcα2-3Galβ1-3GalNAc (sialyl TF Ag) moieties (Table I). In vitro proteolysis with immunoproteasomes was performed until the reference substrate, a non-glycosylated 100-meric repeat peptide, was quantitatively degraded. The fragments were chromatographed by HPLC for quantification and identified either by MALDI-TOF mass spectrometry via their molecular mass ions or by ESI-qtof-MS/MS via

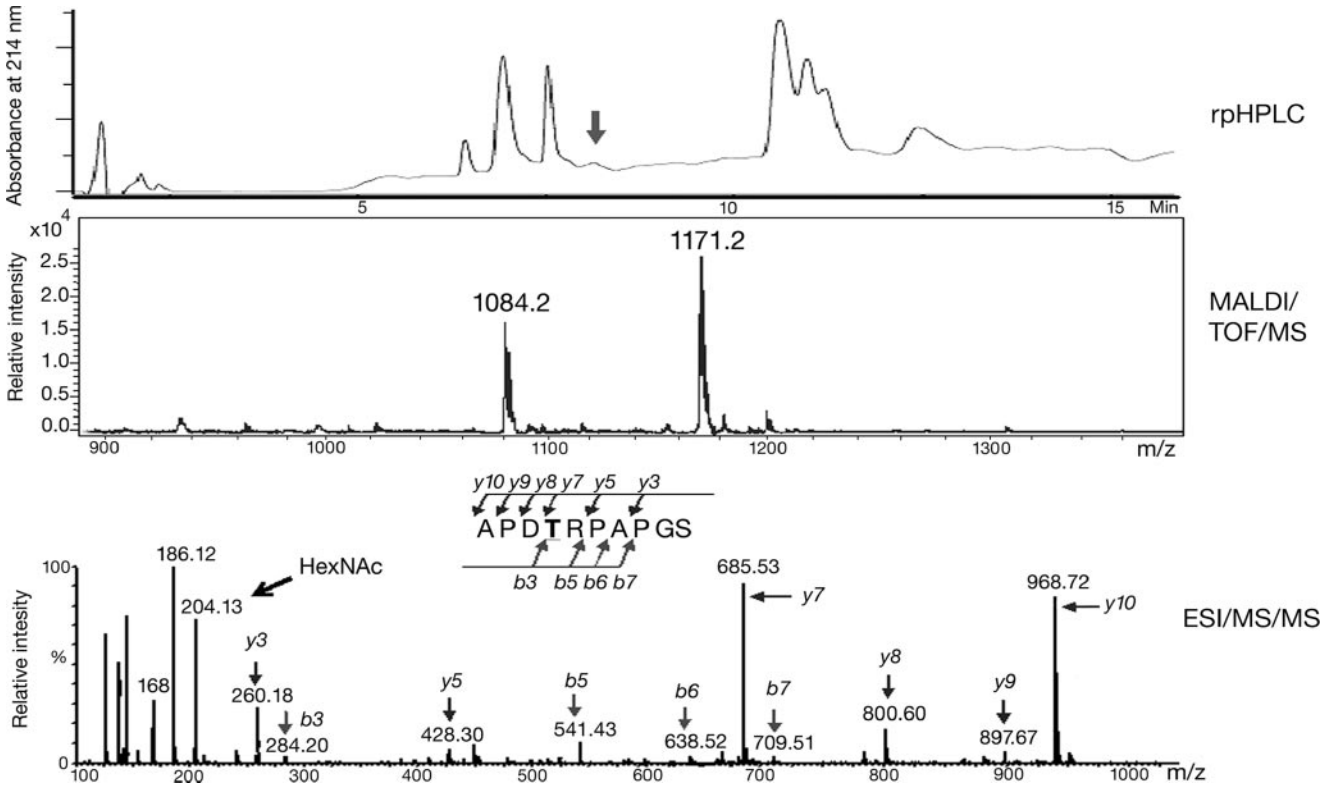

FIGURE 3. Analysis of processing products of GP3 glycopeptide by reverse-phase HPLC, MALDI-MS, and LC-ESI-MS/MS. *Upper panel*, The peptide digest was fractionated on a reverse-phase ultrasphere-C18 column. *Middle panel*, The fraction marked by an arrow was analyzed by MALDI-MS. *Lower panel*, Collision-induced dissociation experiments were performed in positive ion ESI-MS/MS of the HPLC fraction (arrow) providing sequence information via y_i and b_i fragment ions supporting the decapeptide APDT (GalNAc) RPAPGS (MH m/z 1171.2).

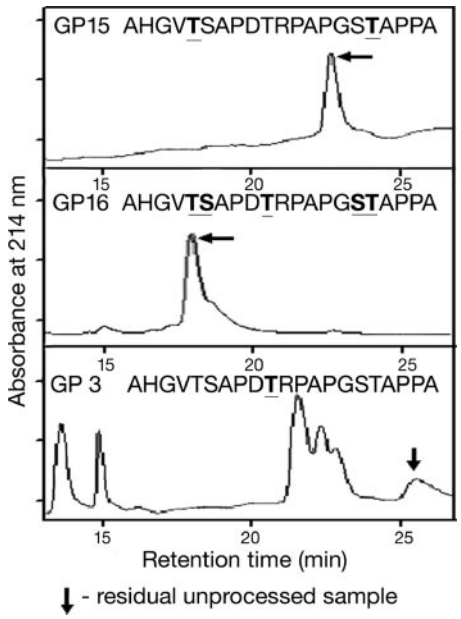

FIGURE 4. Influence of site-specific *O*-glycosylation on processing efficiency. Glycosylated positions are marked by bold underlined letters in the amino acid sequence. Glycopeptides GP15, GP16, and GP3 were digested by immunoproteasomes and analyzed by reverse-phase HPLC. Glycopeptide GP15 glycosylated at both major digestion motifs as well as GP16, glycosylated at all putative glycosylation sites, were largely resistant to proteolysis. The digest of GP3 contained a small amount of unprocessed peptide and high amounts of short- and middle-length fragments.

their b_i or y_i fragment ions (Fig. 3). Two independent assays for most of the substrates showed close similarity with respect to proteolytic fragmentation patterns and relative amounts of fragments.

Digestion of nonglycosylated peptides was independent of their sizes (21-mer to 100-mer) and occurred at high rates irrespective of sequence variations at the immunodominant motif (DT > ES) resulting in quantitative cleavage of the substrates during 24 h. During the same time period, all glycopeptide substrates showed more or less reduced degradation rates that varied from <1 to 90% (Table I). The heavily *O*-glycosylated 100-mer (GP1) carrying 15 GalNAc moieties (three per repeat) was revealed as the poorest substrate with a degradation rate of <1%, while the 20-mer glycosylated at three nearly identical positions (GP11) was degraded much faster (~65%). No direct correlation between number of glycan chains per repeat and proteolysis efficiency was revealed, because the corresponding 20-mer with one or two GalNAc moieties were degraded more slowly (GP9, GP10, GP12) or at comparable rates (GP13, GP14). Strikingly, the 20-meric glycopeptides GP15 and GP16 with another starting motif and two or five GalNAc residues were fully resistant to immunoproteasome proteolysis pointing to site-specific effects of *O*-glycosylation (Fig. 4).

In another series of experiments, we addressed the question of whether elongated glycans, like the disaccharide Gal1-3GalNAc or its sialylated derivative NeuAc2-3Gal1-3GalNAc could have negative effects on processing rates compared with substrates glycosylated with the core sugar GalNAc. Identical 21-meric peptides with AHG starting motif (GP2-GP4; GGP1-GGP3; SGGP1-SGGP5), monosubstituted with any of the three glycans, were assayed and revealed higher degradation rates for the disaccharide substituted peptides compared with their monosaccharide substituted reference peptides. Unexpectedly, the replacement of GalNAc by Gal1-3GalNAc at the same peptide position increased the degradation rate by 30%. In contrast, sialylated glycopeptides were processed at a very low rate, comparable to the densely glycosylated GP1 and GP16 substrates.

Together, these data indicate that if glycopeptide Ags get access to immunoproteasomes via cross-presentation mechanisms, they can be processed by these protease complexes quite effectively. We further learned that not the absolute number, but the sites of glycan substitution had strong effects on immunoproteasome processing.

Glycans modulate cleavage site patterns

After establishing human immunoproteasomes as effectively processing even *O*-glycosylated MUC1 repeat peptides, we wanted to elucidate potential effects of *O*-glycosylation exerted on proteasomal cleavage sites. For this purpose, the digestion products were identified by MS and quantified in a combined chromatographic and mass spectrometric approach to determine the frequencies of cleavage at each peptide bond of the substrates. Between two independent digests of the same peptide, no difference in cleavage patterns was observed.

The most frequently used cleavage sites in the nonglycosylated 100-mer P1 are located within or adjacent to the motif S-A-P contributing to 50% of all generated peptides (Fig. 5). This compares to <1% of peptide products contributed by other sites and confirms previous reports claiming that the relative usage of processing sites can differ substantially. A second more frequently used cleavage region is the G-S-T motif contributing to ~9% of all peptides released from the 100-mer. These site preferences of proteasomal cleavage are retained also with shorter substrate peptides as revealed for the nonglycosylated 20-mer: S-A-P releasing ~22% and G-S-T ~16% of all peptides. Interestingly, the major processing regions overlap with the preferred substrate positions of the ubiquitously expressed polypeptide GalNAc transferases

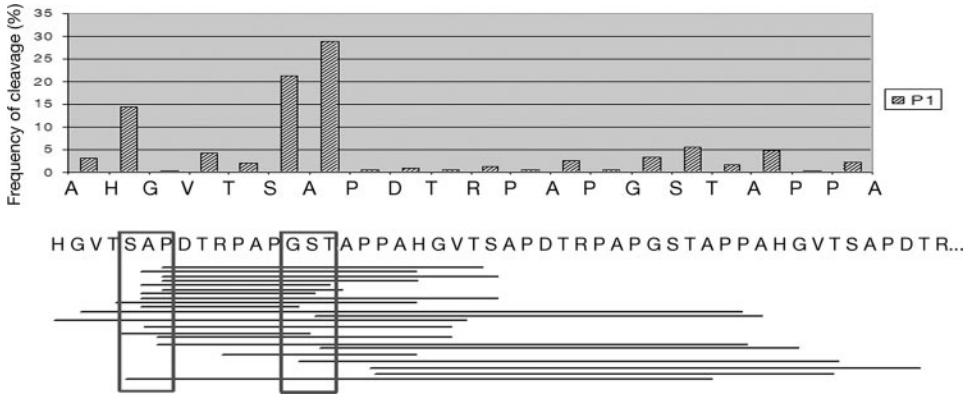

FIGURE 5. Frequency of cleavage at peptide bonds of P1 peptide. *Upper panel*, The digest of the 100-meric P1 peptide was analyzed by HPLC and MALDI-MS and frequencies of cleavage site usage were calculated as presented in the histogram. *Lower panel*, The most prominent peptide fragments were presented as horizontal bars. The boxes mark the major cleavage regions SAP and GST within the repeat peptide.

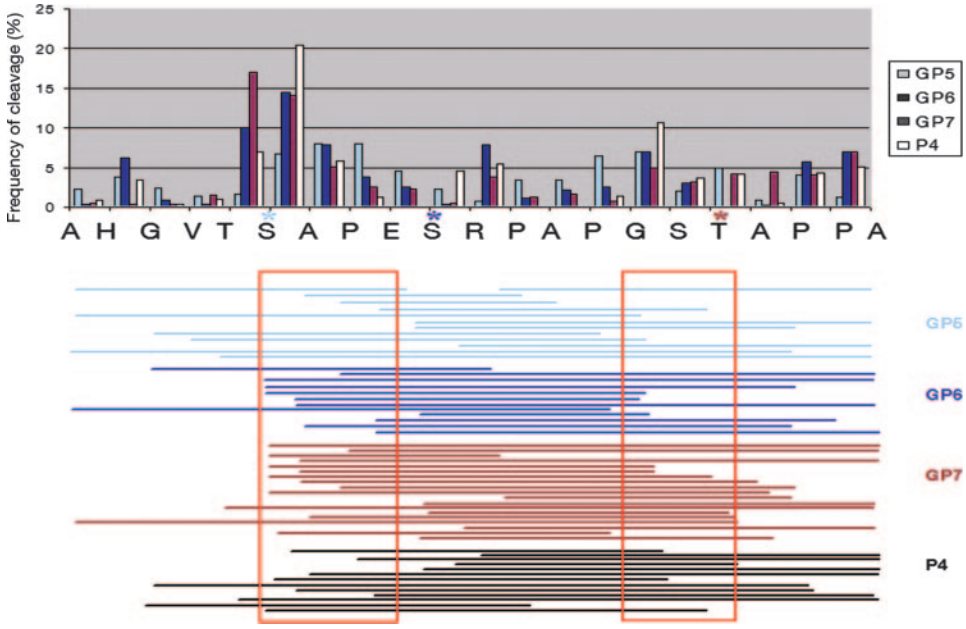

FIGURE 6. Frequency of peptide bond cleavage in dependence on glycosylation positions. *Upper panel*, The activity of immunoproteasomes in the main processing regions SAP and GST is modulated by glycans in adjacent or proximal positions. Presence of glycans at Thr in the VTS motif reduces the cleavage frequency between T-S and S-A in the SAP region (light blue bars). Glycosylation at the ESR motif does not change the immunoproteasomal activity (dark blue bars). GalNAc at Thr within the GST motif in GP7 reduces the processing within this region (red bars). *Lower panel*, most frequent peptide fragments detected in digestion mixtures of glycopeptides GP5, GP6, GP7. The boxes mark the major cleavage regions SAP and GST within the repeat peptide.

ppGalNAc-T1 and -T2 and are generally glycosylated in the native MUC1 glycoforms (29, 30).

Expectedly, the immunoproteasome cleavage rates within these two regions were strongly dependent on the position of glycosylation (Fig. 6). Glycans linked to Thr adjacent to the SAP motif reduced the relative frequencies of cleavage within the motif to ~8% (refer to glycopeptide GP5 and the nonglycosylated reference peptide P4 in Fig. 3). Cleavage frequencies at the GST region remained largely unchanged upon glycosylation of Ser/Thr within the (T)SAP motif. Vice versa, glycosylation of Thr within the GST motif reduced cleavage rates at this region to almost 3%, while the cleavage within the SAP region remained largely unaffected compared with the reference peptide (refer to glycopeptide GP7).

From these data it can be concluded that the cleavage rates at the preferred sites of the repeat peptide are controlled by the positions of *O*-linked glycans. Precisely, those positions in close proximity to *O*-glycosylation are strongly affected, while the respective position in some distance to the glycan shows no reduction in cleavage rates. Simultaneous presence of glycans at both preferred regions of cleavage prevents immunoproteasomal proteolysis almost completely (GP15, GP16, GP1). Presence of glycans at the DTR motif located proximal to both preferred cleavage sites did not change the cleavage patterns (refer to P4 vs GP6 in Fig. 3). Consequently, a different set of peptides will be released from differentially glycosylated peptides.

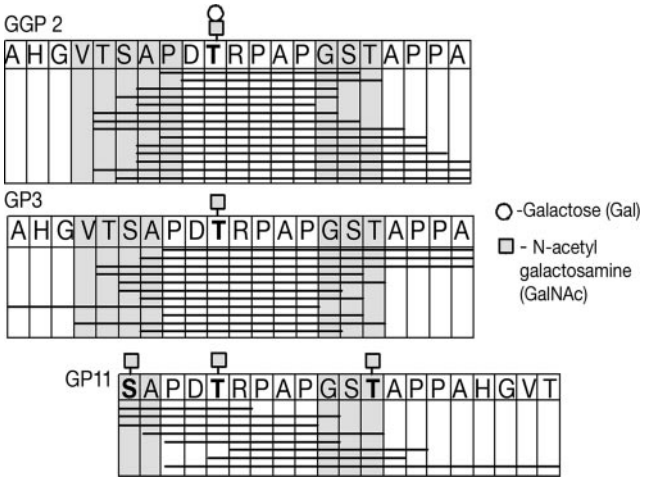

FIGURE 7. Major fragments of glycopeptide substrates with different starting motifs within the repeat peptide and different glycan chains. Fragments generated from all three glycopeptides GGP2, GP3, and GP11 were generated by cleavage within or adjacent to the SAP and GST motifs, regardless of the glycosylation type (Gal-GalNAc in GGP2 vs GalNAc in GP3) and starting motifs (AHG vs SAP in GP3 or GP11). Glycosylation positions are indicated by □ (GalNAc), and ○ (Gal).

In an additional series of experiments, we addressed the question of whether the shift in the peptide-starting motif could have an influence on the proteasomal site specificity. Glycopeptides with AHG- or SAP-starting motifs were assayed and the released peptide products indicated identical cleavage site specificity (Fig. 7).

The specificity of cleavage is also not influenced by introduction of elongated glycans. The replacement of a monosaccharide (GalNAc) by a disaccharide (Gal1-3GalNAc) should considerably increase the sterical shielding of the peptide and reduce cleavage rates at proximal sites. Sequence identical pairs of peptides (GP3 and GGP2 as well as GP8 and GGP4) monosubstituted with GalNAc or Gal-GalNAc were assayed and revealed no difference in digestion patterns.

From these findings, we learned that glycosylation negatively influences processing in its close proximity and this effect is observed for both the mono- and disaccharide substituted glycopeptides. Moreover, major glycosylation sites within the MUC1 repeat domain are found in close proximity to the preferred cleavage sites of immunoproteasomes and prevent effective processing of native MUC1 glycoforms. Glycosylation-dependent block of proteasomal digestion within the main processing regions results in cleavage at new or less preferred substrate sites.

Discussion

This study was undertaken to address the questions of whether 1) immunoproteasomes involved in MHC class I-related cross-presentation mechanisms are able to cleave mucin-type *O*-glycosylated peptides and 2) in which way *O*-linked glycans influence the pattern of cleavage sites in such Ags. The model glycoprotein MUC1 represents one of the favorite target Ags in anticancer strategies in diagnostic and therapeutic respect. Numerous attempts

were made in animal models and in humans to induce humoral and cellular responses to defeat MUC1-positive tumors. One shortcoming in these studies was the obvious discrepancy between the nonglycosylated MUC1 Ag used in experimental models and glycosylated MUC1 Ag triggering weak immune response in cancer patients.

The intuitive assumption that *O*-linked glycans should disturb processing rather broadly and therefore should be removed before proteolytic cleavage of the protein was falsified by recent evidence demonstrating that even complex *O*-glycans survive the processing machinery and appear on the cell surface of DCs in MHC class II complexes as structural components of glycopeptides (12). In the MHC class I pathway, nucleocytosolic glycoproteins were found presented as a small fraction of MHC-bound GlcNAc-*O*-peptides (26, 27). For the mucin-type *O*-glycosylated ectodomain of MUC1, no such evidence was provided on the cellular level. The reason for that could be found in the low efficiency of cross-presentation mechanisms, which mediate proteolysis of ectodomain epitopes and their presentation by MHC class I proteins. One of these mechanisms involves endosomal uptake and escape of the Ag into the cytosol, where it gets access to immunoproteasomes. This process apparently works at low levels, because attempts made by different groups to isolate and structurally characterize class I-bound MUC1 (glyco)peptides generated by cellular processing in DCs were unsuccessful (A. Vlad and O. J. Finn; T. Ninkovic and F. G. Hanisch, unpublished observations).

This study provides for the first time in vitro evidence on the capacities of purified immunoproteasomal complexes to fragment *O*-glycosylated peptides of the MUC1 tandem repeat domain. We could demonstrate the dependency of effective proteolysis on the buffer conditions, and confirmed the absence of contaminating proteases. Human immunoproteasomes were revealed as effective machines for the processing of *O*-glycosylated peptides. However, the cleavage rates are strongly dependent on the sites of glycan substitution. This finding contrasts with the respective nonglycosylated peptides, which were quantitatively degraded. Irrespective of the starting motif within the repeat or the peptide lengths, all peptides showed a constant cleavage pattern with preferred sites at the SAP and GST regions. Over 50% of peptide products were generated from proteolysis at these sites yielding a panel of prominent 8- to 11-mer starting with SAP, APD, or PDT. The actual cleavage patterns overlap partially with the predictions from NetChop 3.0 (Fig. 8). Glycans influence this cleavage pattern in several ways. First, they suppress or block adjacent cleavage sites already on the monosaccharide level (Fig. 8). Second, they change the processing patterns by making poor substrate sites more effective. Third, the elongation of glycans from mono- to disaccharides does not necessarily reduce cleavage rates (it can even increase it). However, sialoglycopeptides carrying one or more negatively charged sialic acid residues were poor substrates for immunoproteasomes. In particular, only SGGP4, a sialoglycopeptide with two NeuAc2-3Gal1-3GalNAc trisaccharides linked to GSTA, was cleaved at the preferred SAP motif. All other sialoglycopeptides carried at least one sialyltrisaccharide at (T)SAP, which completely inhibited cleavage at this motif. It is evident that the more bulky and charged modifications affect entrance of the substrate into the proteasomal cylinder and/or the accessibility of the preferred peptide bonds to the proteolytically active enzymes. In summary, the findings of this study demonstrate for the first time that immunoproteasomes are principally able to cleave mucin-type *O*-glycosylated peptides and specifically show how immunoproteasomes deal with *O*-glycopeptides of the MUC1 repeat domain. Potential limitations of this study arising from a minor admixture of constitutive immunoproteasomes (c20S) can be regarded as not significant. According to preliminary data on MUC1 repeat peptide processing by c20S (T. Ninkovic and F.-G. Hanisch, unpublished results), their cleavage preferences overlap largely with those of the i20S preparation used in this study.

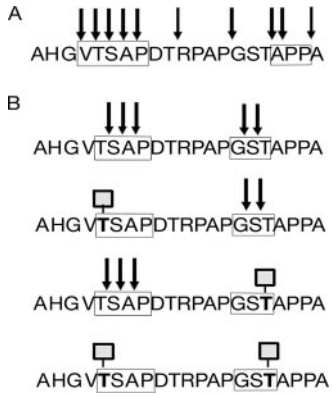

FIGURE 8. The processing pattern of MUC1 tandem repeat peptides predicted by NetChop 3.0. *Upper panel*, The predicted cleavage sites within the MUC1 repeat peptide (*A*) and the lower to experimentally determined cleavage sites (*B*). According to bioinformatic prediction of cleavage sites performed by NetChop 3.0, major cleavage regions of nonglycosylated MUC1 tandem repeat peptides overlap with the experimentally determined patterns. Digestion of nonglycosylated and glycosylated MUC1 tandem repeat peptides by immunoproteasomes revealed SAP and GST as main digestion regions, which are affected by adjacent glycosylation (□, GalNAc; ○, Gal).

The above-summarized evidences on glycosylation-dependent restrictions of immunoproteasome processing can be regarded as one of several possible explanations of why native MUC1 represents a poor immunogen for CTL induction. Previous structural studies have shown that low-density glycoforms of the normal, lactation-associated mucin exhibit a random substitution of all five potential glycosylation sites with an average density of 2.5 glycans per repeat (31). By contrast, the tumor-associated, high-density glycoforms with four to five glycans per repeat (32) does not expose longer stretches of nonglycosylated core peptide. Accordingly, Thr/Ser residues within or adjacent to the preferred immunoproteasomal cleavage motifs SAP and GST are substituted in 95% of the repeats. The Thr adjacent to the SAP motif and the Thr within the GST motif are the preferred substrate sites of the ubiquitous polypeptide GalNAc-transferases ppGalNAc-T1 and -T2 (30) making cancer-associated MUC1 a poor substrate of immunoproteasomes. Accordingly, APCs in tumor patients that endocytosed tumor-secreted or shed MUC1 are unable to present these glycosylated epitopes in the MHC class I pathway for the activation of cytotoxic T cells. Vaccination with designed chemically synthesized MUC1 glycopeptides could overcome this problem.

Glycopeptides used in this study represent true proteasomal substrates with relevance in the tumor therapeutic context. Due to an underexpression of the core 2 β6-GlcNAc transferases and an overexpression of α3-sialyltransferase in breast cancer cells, Tn (GalNAc), TF (Gal1-3GalNAc), and their sialylated derivatives are the predominating glycans on tumor-associated MUC1 glycoforms (3). Irrespective of how these glycopeptides get access to immunoproteasomes, the glycan moieties of the peptides should remain stable on their endosomal and cytosolic routes. Tn and TF glycopeptides had been shown to survive endosomal processing (12) and the cytosol does not contain glycosidases active on this type of glycans, which is regularly found on proteins with a secretory or extracellular topology.

FIGURE 9. MUC1 domain topology and known CTL epitopes. Bolded and lined sequences correspond to established MHC-restricted CTL epitopes, bolded sequences to MHC-unrestricted CTL epitopes. The PDTRP and PESRP sequences within the tandem repeat domain represent also immunodominant B cell epitopes (33). Preferred immunoproteasomal cleavage regions in the tandem repeat are marked by triple arrows. The N- to C-terminal MUC1 domain topology is: S, signal peptide; N, N-terminal domain; D, degenerate repeats; R, tandem repeat domain containing regular and variant (italic amino acids) sequences; P, SEA (sperm protein-enterokinase-agrin) domain containing the MUC1-processing site; M, transmembrane domain; C, cytosolic domain.

Among the octa- to undecapeptides generated as the major processing products from MUC1 (glyco)peptides by immunoproteasomal cleavage two series were identified that overlapped with the sequences of known CTL epitopes (Fig. 9). The first series covered the MHC-unrestricted epitope (A)PDTRP(A) containing the DTR motif (5), while the second overlapped with the HLA-A11- (and to a lesser extent HLA-A1, -A2.1, and -A3) restricted epitope identical with the sequence STAPPAHGV(T) (6).

General conclusions drawn from this in vitro study should aid the design of efficient vaccines for the induction of CTL responses to the glycosylated target on MUC1-positive tumor cells. To enable efficient processing by immunoproteasomes, the antigenic glycopeptide(s) in a synthetic vaccine formulation should fulfill specific requirements, i.e., a site-specific *O*-glycosylation restricted to the DTR motif and a substitution with core-type *O*-glycan moieties, GalNAc (Tn Ag) or Galβ1-3GalNAc (TF Ag). Sialylated extensions of these core glycans or glycans at other sites of the repeat peptide reduce or block the processing by immunoproteasomes and certainly prevent the formation of fragments fitting to the binding groove of MHC class I proteins. Recent work has revealed that some decameric immunoproteasomal-processing products of glycopeptides bind with equal strength to MHC class I as their nonglycosylated counterparts. Moreover, human DCs pulsed with these glycosylated decamers were able to induce a CTL response (T. Ninkovic, L. Kinarsky, K. Engelmann, V. Pisarev, S. Sherman, O. Finn, F.-G. Hanisch, manuscript in preparation). Combined with forced adjuvant strategies and technical improvements allowing the ready uptake of Ag into the cytosol (as lipid-conjugates in liposomes, in linkage to peptide mediators like penetratin, complexes with or fused to heat shock protein, as cargo of virosomes), the immunization with a panel of site-specifically designed glycopeptides should open access to a hitherto largely unexplored repertoire of glycopeptide-specific CTLs.

Acknowledgments

MS was performed in the Central Bioanalytics of the Center for Molecular Medicine (Cologne, Germany). We acknowledge the support by Dr. Stefan Müller in the performance of ESI-MS. We also thank Prof. Hans Paulsen (Institute of Organic Chemistry, University of Hamburg, Hamburg, Germany) for kindly providing synthetic glycopeptides.

Disclosures

The authors have no financial conflict of interest.

References

1. Gendler, S. J., A. P. Spicer, E. N. Lalani, T. Duhig, N. Peat, L. Pemberton, M. Boshell, and J. Taylor-Papadimitriou. 1991. Structure and biology of a carcinoma-associated mucin, MUC1. *Am. Rev. Respir. Dis.* 144: 42–47.
2. von Mensdorff-Pouilly, S., E. Petrakou, P. Kenemanns, K. van Uffelen, A. A. Verstraeten, F. G. Snijdewint, G. J. van Kamp, D. J. Schol, C. A. Reis, M. R. Price, et al. 2000. Reactivity of natural and induced human antibodies to MUC1 mucin with MUC1 peptides and *N*-acetylgalactosamine (GalNAc) peptides. *Int. J. Cancer* 86: 702–712.
3. Hanisch, F.-G., and S. Müller. 2000. MUC1: the polymorphic appearance of a human mucin. *Glycobiology* 10: 439–449.
4. Engelmann, K., S. E. Baldus, and F.-G. Hanisch. 2001. Identification and topology of variant sequences within individual repeat domains of the human epithelial tumor mucin MUC1. *J. Biol. Chem.* 276: 27764–27769.
5. Jerome, K. R., D. L. Barnd, K. M. Bendt, C. M. Boyer, J. Taylor-Papadimitriou, I. F. McKenzie, R. C. Bast, and O. J. Finn. 1991. Cytotoxic T-lymphocytes derived from patients with breast adenocarcinoma recognize an epitope present on the protein core of a mucin molecule preferentially expressed by malignant cells. *Cancer Res.* 51: 2908–2916.
6. Domenech, N., R. A. Henderson, and O. J. Finn. 1995. Identification of an HLA-A11-restricted epitope from the tandem repeat domain of the epithelial tumor antigen mucin. *J. Immunol.* 155: 4766–4774.
7. Brossart, P., K. S. Heinrich, G. Stuhler, L. Behnke, V. L. Reichardt, S. Stevanovic, A. Muhm, H.-G. Rammensee, L. Kanz, and W. Brugger. 1999. Identification of HLA-A2-restricted T-cell epitopes derived from the MUC1 tumor antigen for broadly applicable vaccine therapies. *Blood* 93: 4309–4317.
8. Heukamp, L. C., S. H. van der Burg, J. W. Drijfhout, C. J. Melief, J. Taylor-Papadimitriou, and R. Offringa. 2001. Identification of three non-VNTR MUC1-derived HLA-A*0201-restricted T-cell epitopes that induce protective anti-tumor immunity in HLA-A2/K(b)-transgenic mice. *In. J. Cancer* 91: 385–392.
9. Pisarev, V. M., L. Kinarsky, T. Caffrey, F.-G. Hanisch, S. Sanderson, M. A. Hollingsworth, and S. Sherman. 2005. T-cells recognize PD(N/T)R motif common in a variable number of tandem repeat and degenerate repeat sequences of MUC1. *Int. Immunopharmacol.* 5: 315–330.
10. Hiltbold, E. M., M. D. Alter, P. Ciborowski, and O. J. Finn. 1999. Presentation of MUC1 tumor antigen by class I MHC and CTL function correlate with the glycosylation state of the protein taken up by dendritic cells. *Cell. Immunol.* 194: 143–149.
11. Hiltbold, E. M., A. Vlad, P. Ciborowski, S. C. Watkins, and O. J. Finn. 2000. The mechanism of unresponsiveness to circulating tumor antigen MUC1 is a block in intracellular sorting and processing by dendritic cells. *J. Immunol.* 165: 3730–3741.

12. Vlad, A., S. Müller, M. Cudic, H. Paulsen, L. Otvos, F.-G. Hanisch, and O. J. Finn. 2002. Complex carbohydrates are not removed during processing of glycoproteins by dendritic cells: processing of tumor antigen MUC1 glycopeptides for presentation to major histocompatibility complex class II-restricted T cells. *J. Exp. Med.* 196: 1435–1446.
13. Hanisch, F.-G., T. Schwientek, M. S. von Bergwelt-Baildon, J. L. Schultze, and O. J. Finn. 2003. *O*-linked glycans control glycoprotein processing by antigen-presenting cells: a biochemical approach to the molecular aspects of MUC1 processing by dendritic cells. *Eur. J. Immunol.* 33: 3242–3254.
14. Apostolopoulos, V., E. Yuriev, P. A. Ramsland, J. Halton, C. Osinski, W. Li, M. Plebanski, H. Paulsen, and I. F. C. McKenzie. 2003. A glycopeptide in complex with MHC class I uses the GalNAc residue as an anchor. *Proc. Natl. Acad. Sci. USA* 100: 15029–15034.
15. Stepensky, D., E. Tzehoval, E. Vadai, and L. Eisenbach. 2006. *O*-glycosylated versus non-glycosylated MUC1-derived peptides as potential targets for cytotoxic immunotherapy of carcinoma. *Clin. Exp. Immunol.* 143: 139–149.
16. Hearn, A. R., L. de Haan, A. J. Pemberton, T. R. Hirst, and A. J. Rivett. 2004. Trafficking of exogenous peptides into proteasome-dependent major histocompatibility complex class I pathway following enterotoxin B subunit-mediated delivery. *J. Biol. Chem.* 279: 51315–51322.
17. Seifert, U., C. Maranon, A. Shmueli, J. F. Desoutter, L. Wesoloski, K. Janek, P. Henklein, S. Diescher, M. Andrieu, H. de la Salle, et al. 2003. An essential role for tripeptidyl peptidase in the generation of an MHC class I epitope. *Nat. Immunol.* 4: 375–379.
18. Chen, L., and M. Jondal. 2004. Endolysosomal processing of exogenous antigen into major histocompatibility complex class I-binding peptides. *Scand. J. Immunol.* 59: 545–552.
19. Shen, L., L. J. Sigal, M. Boes, and K. L. Rock. 2004. Important role of cathepsin S in generating peptides for TAP-independent MHC class I crosspresentation in vivo. *Immunity* 21: 155–165.
20. Goldberg, A. L., S. J. Elledge, and J. W. Harper. 2001. The cellular chamber of doom. *Sci. Am.* 284: 68–73.
21. Tanaka, K., and M. Kasahara. 1998. The MHC class I ligand-generating system: roles of immunoproteasomes and the interferon-γ-inducible proteasome activator PA28. *Immunol. Rev.* 163: 161–176.
22. Boes, B., H. Hengel, T. Ruppert, G. Multhaup, U. H. Koszinowski, and P. M. Kloetzel. 1994. Interferon γ stimulation modulates the proteolytic activity and cleavage site preference of 20S mouse proteasomes. *J. Exp. Med.* 179: 901–909.
23. Suzuki, T. 2005. A simple, sensitive in vitro assay for cytoplasmic deglycosylation by peptide: *N*-glycanase. *Methods* 35: 360–365.
24. Skipper, J. C., R. C. Hendrickson, P. H. Gulden, V. Brichard, A. Van Pel, Y. Chen, J. Shabanowitz, T. Wolfel, C. L. Slingluff, T. Boon, et al. 1996. An HLA-A2-restricted tyrosinase antigen on melanoma cells results from posttranslational modification and suggests a novel pathway for processing of membrane proteins. *J. Exp. Med.* 183: 527–534.
25. Haurum, J. S., G. Arsequell, A. C. Lellouch, S. Y. Wong, R. A. Dwek, A. J. McMichael, and T. Elliott. 1994. Recognition of carbohydrate by major histocompatibility complex class I-restricted, glycopeptide-specific cytotoxic T lymphocytes. *J. Exp. Med.* 180: 739–744.
26. Kastrup, I. B., S. Stevanovic, G. Arsequell, G. Valencia, J. Zeuthen, H.-G. Rammensee, T. Elliott, and J. S. Haurum. 2000. Lectin purified human class I MHC-derived peptides: evidence for presentation of glycopeptides in vivo. *Tissue Antigens* 56: 129–135.
27. Haurum, J. S., I. B. Høier, G. Arsequell, A. Neisig, G. Valencia, J. Zeuthen, J. Neefjes, and T. Elliott. 1999. Presentation of cytosolic glycosylated peptides by human class I major histocompatibility complex molecules in vivo. *J. Exp. Med.* 190: 145–150.
28. Tenzer, S., L. Stotze, B. Schönfisch, J. Dengjel, M. Müller, S. Stefanovic, H.-G. Rammensee, and H. Schild. 2004. Quantitative analysis of prion-protein degradation by constitutive and immuno-20S proteasomes indicates differences correlated with disease susceptibility. *J. Immunol.* 172: 1083–1091.
29. Hanisch, F. G., S. Müller, H. Hassan, H. Clausen, N. Zachara, A. A. Gooley, H. Paulsen, K. Alving, and J. Peter-Katalinic. 1999. Dynamic epigenetic regulation of initial *O*-glyco-sylation by UDP-*N*-acetylgalactosamine: peptide *N*-acetylgalactosaminyltransferases: site-specific glycosylation of MUC1 repeat peptide influences the substrate qualities at adjacent or distant Ser/Thr positions. *J. Biol. Chem.* 274: 9946–9954.
30. Hanisch, F. G., C. A. Reis, H. Clausen, and H. Paulsen. 2001. Evidence for glycosylation-dependent activities of polypeptide *N*-acetylgalactosaminyltransferases rGalNAc-T2 and -T4 on mucin glycopeptides. *Glycobiology* 11: 731–740.
31. Müller, S., S. Goletz, N. Packer, A. A. Gooley, A. M. Lawson, and F.-G. Hanisch. 1997. Localization of *O*-glycosylation sites on glycopeptide fragments from lactation-associated MUC1. *J. Biol. Chem.* 272: 24780–24793.
32. Müller, S., K. Alving, J. Peter-Katalinic, N. Zachara, A. A. Gooley, and F.-G. Hanisch. 1999. High density *O*-glycosylation on tandem repeat peptide from secretory MUC1 of T47-D breast cancer cells. *J. Biol. Chem.* 274: 18165–18172.
33. von Mensdorff-Pouilly, S., L. Kinarsky, K. Engelmann, S. E. Baldus, R. H. Verheijen, M. A. Hollingsworth, V. Pisarev, S. Sherman, and F.-G. Hanisch. 2005. Sequence-variant repeats of MUC1 show higher conformational flexibility, are less densely *O*-glycosylated and induce differential B lymphocyte responses. *Glycobiology* 15: 735–746.